Supporting Information

QM/MM Modeling of Vibrational Polariton Induced Energy Transfer and Chemical Dynamics

Tao E. Li* and Sharon Hammes-Schiffer*

Department of Chemistry, Yale University, New Haven, Connecticut, 06520, USA

E-mail: tao.li@yale.edu; sharon.hammes-schiffer@yale.edu

1. Additional simulation details

In this work, a molecular system of 16 $Fe(CO)_5$ molecules is coupled to a cavity mode with frequency $\omega_c = 2018$ cm^{-1}. The cavity mode contains two (x and y) polarization directions. The auxiliary mass of the cavity photon mode is set as $m_c = m_{k,\lambda} = 1$ a.u. The $Fe(CO)_5$ molecules are described by DFT with the BP86[S1] functional, which has been used extensively for $Fe(CO)_5$,[S2,S3] and the def2-mSVP[S4] basis set. For each individual $Fe(CO)_5$ molecule, the surrounding solvent environment is modeled by 50 n-dodecane molecules using the OPLS-AA[S5] force field. The QM/MM interaction is treated with a two-layer ONIOM model under mechanical embedding,[S6] which is expected to be reasonable for this relatively non-polar solvent, as implemented in Q-Chem. In the QM/MM calculations, the partial charges and Lennard–Jones parameters of $Fe(CO)_5$ are defined as follows: $Q_{Fe} = 0.0238$ $|e|$, $\sigma_{Fe} = 3.11$ Å, $\epsilon_{Fe} = 0.2868$ kcal/mol; $Q_C = 0.07124$ $|e|$, $\sigma_C = 3.30$ Å, $\epsilon_C = 0.6597$ kcal/mol; $Q_O = -0.0760$ $|e|$, $\sigma_O = 3.09$ Å, $\epsilon_O = 0.1434$ kcal/mol. The Lennard–Jones parameters were chosen from the OPLS-AA force field, and the partial charges were calculated by the Hirshfeld population analysis[S7] from the QM calculation for a single $Fe(CO)_5$ molecule at its optimized geometry. Although the Hirshfeld partial charges of C and O atoms at equatorial and axial locations are slightly different, here, due to the existence of pseudorotation, Q_C (Q_O) is defined as the average value of the five C (O) Hirshfeld partial charges.

Because the n-dodecane vibrational frequencies differ significantly from the CO vibrations in $Fe(CO)_5$, we chose to turn off the cavity-solvent interaction throughout the calculations presented in this manuscript, i.e., in Eq. (6), the MM contribution to the dipole moment and dipole derivatives is set to zero.

The initial geometry of the QM/MM system was prepared as follows. The configuration of one $Fe(CO)_5$ molecule surrounded by 50 n-dodecane molecules was prepared in a cubic cell of length 13.4 Å by PACKMOL.[S8] This initial configuration, with initial velocities chosen according to a Maxwell–Boltzmann distribution at 300K, was equilibrated for 20 ps under an NVT (constant number of particles, volume, and temperature) ensemble attached to a

Langevin thermostat with a friction lifetime of 100 fs. From this 20 ps NVT trajectory, 16 configurations were taken from $t = 12.5$ ps to $t = 20$ ps with an inverval of 0.5 ps. Each of these 16 configurations, which contain one $Fe(CO)_5$ molecule plus 50 n-dodecane molecules, was rotated randomly with PACKMOL, and the combination of these 16 configurations formed the initial state of the VSC simulations. Because the combined molecular configurations in this initial state may have a permanent dipole moment, in order to ensure the initial potential energy for each photon coordinate is thermally equilibrated, we set the initial photonic coordinates to be $\widetilde{\widetilde{q}}_{c,\lambda} = \sqrt{k_B T/m_c\omega_c^2} - \widetilde{\varepsilon}\widetilde{d}^{sub}_{g,\lambda}/m_c\omega_c$, so that the potential energy in Eq. (1b) for each photon coordinate was $k_B T/2$.

With the initial QM/MM molecular system configuration prepared as described above, we simulated the coupled cavity-molecular system for 1 ps to calculate the polariton spectrum. The initial velocities of all particles (photons + nuclei) were assigned according to the Maxwell–Boltzmann distribution at 300K. This simulation was propagated for 1 ps under an NVE ensemble. Note that the cavity mode equation of motion given in Eq. (3b) depends on the total dipole moment summed over all the independent molecular systems at each time step, which therefore must be propagated in parallel. When calculating the polariton spectrum, the Fourier transform of the autocorrelation function of the photonic coordinates is calculated:

$$C(\omega) = \frac{\omega^2}{2\pi}\int_{-\infty}^{+\infty} dt\ e^{-i\omega t}\left\langle \sum_{\lambda=x,y} \widetilde{\widetilde{q}}_{c,\lambda}(0)\widetilde{\widetilde{q}}_{c,\lambda}(t)\right\rangle \tag{S1}$$

With the same initial QM/MM molecular configurations as used to calculate the polariton spectrum, we propagated a nonequilibrium simulation of the coupled cavity-molecular system under a Gaussian pulse excitation for 2.5 ps. The Gaussian pulse is defined in Eq. (7). This Gaussian pulse interacts with the x-polarized cavity mode and can selectively excite the UP or the LP when the frequency is set as $\omega = \omega_{LP}$ or $\omega = \omega_{UP}$. The coupling coefficient between the Gaussian pulse and the cavity mode was set as $Q_c = Q_{k,\lambda} = 0.1$ a.u.; see Eq. (3b) and associated text for more details on the definition of $Q_{k,\lambda}$.

During all these QM/MM simulations, an open boundary condition was used. Therefore,

the MM solvent molecules could potentially evaporate when the simulation time becomes very large. However, we checked that during our simulation timescale, i.e, tens of ps, no significant evaporation effect was observed, and each $Fe(CO)_5$ molecule was always surrounded by MM molecules. Hence, the use of the open boundary condition is valid for the current study.

When studying the Berry pseudorotation reaction, for each $Fe(CO)_5$ geometry, we defined the axial CO ligands as the ligand pair with the largest C−Fe−C angle. In Fig. 5, the number of barrier crossings along a 2 ps time span was computed as the sum of the crossings occurring over intervals of 0.5 ps for all of the independent molecular systems. For example, the number of barrier crossings at $t = 1.5$ ps was calculated as the sum of the total number of pseudorotation reactions occurring between $t = 0$ and $t = 0.5$ ps, between $t = 0.5$ and 1.0 ps, and between $t = 1.0$ and $t = 1.5$ ps.

Additional QM simulations excluding the MM solvent molecules were also propagated to calculate the IR spectrum in Figs. 2a,b. These purely QM simulations were propagated in the same manner as the above QM/MM simulations.

2. Hopfield coefficients

We use the following phenomenological three-state model (with $\hbar = 1$) to describe the interaction between the cavity mode and the equatorial and axial vibration modes:

$$\hat{H}_{\text{model}} = \begin{pmatrix} \omega_{\text{c}} & g_{\text{e}} & g_{\text{a}} \\ g_{\text{e}} & \omega_{\text{e}} & 0 \\ g_{\text{a}} & 0 & \omega_{\text{a}} \end{pmatrix}. \tag{S2}$$

Here, ω_{c}, ω_{e}, and ω_{a} denote the frequencies of the cavity mode, the equatorial CO vibrational mode, and the axial CO vibrational mode, respectively; g_{e} and g_{a} denote the corresponding light-matter couplings. The polariton frequencies are defined as the eigen frequencies of

the three-state model. From the Hessian calculation of a single $Fe(CO)_5$ in vacuum at its equilibrium geometry, we obtain $\omega_e = 2010$ cm^{-1}, $\omega_a = 2025$ cm^{-1}, and $g_e/g_a = \sqrt{I_e/I_a} = 1.31$, where I_e and I_a denote the IR intensities of the equatorial and axial vibrational modes, respectively. Given $\omega_c = 2018$ cm^{-1}, we find that when $g_a = 69$ cm^{-1}, the calculated Rabi splitting matches the Rabi splitting in Fig. 2d well. The eigenvalues of our model are $\omega_{LP} = 1903$ cm^{-1}, $\omega_{MP} = 2019$ cm^{-1}, $\omega_{UP} = 2131$ cm^{-1}, and the three eigenvectors are

$$v_{LP} = \begin{pmatrix} -0.70 \\ 0.59 \\ 0.40 \end{pmatrix}, v_{MP} = \begin{pmatrix} -0.06 \\ -0.61 \\ 0.79 \end{pmatrix}, v_{UP} = \begin{pmatrix} 0.71 \\ 0.53 \\ 0.46 \end{pmatrix}. \tag{S3}$$

For each eigenstate, the weights of the photon or two vibrational modes, also known as the Hopfield coefficients, are

$$v_{LP}^2 = \begin{pmatrix} 0.49 \\ 0.35 \\ 0.16 \end{pmatrix}, v_{MP}^2 = \begin{pmatrix} 0.004 \\ 0.37 \\ 0.63 \end{pmatrix}, v_{UP}^2 = \begin{pmatrix} 0.50 \\ 0.28 \\ 0.21 \end{pmatrix}. \tag{S4}$$

Hence, for the UP, the equatorial weight is 0.28, the axial weight is 0.21, and their ratio is 1.33; for the LP, the equatorial weight is 0.35, the axial weight is 0.16, and their ratio is 2.2. The photonic weight in the MP is nearly zero, indicating a very small MP peak in the photonic signal.

3. Polariton dynamics for $Fe(CO)_5$ in vacuum

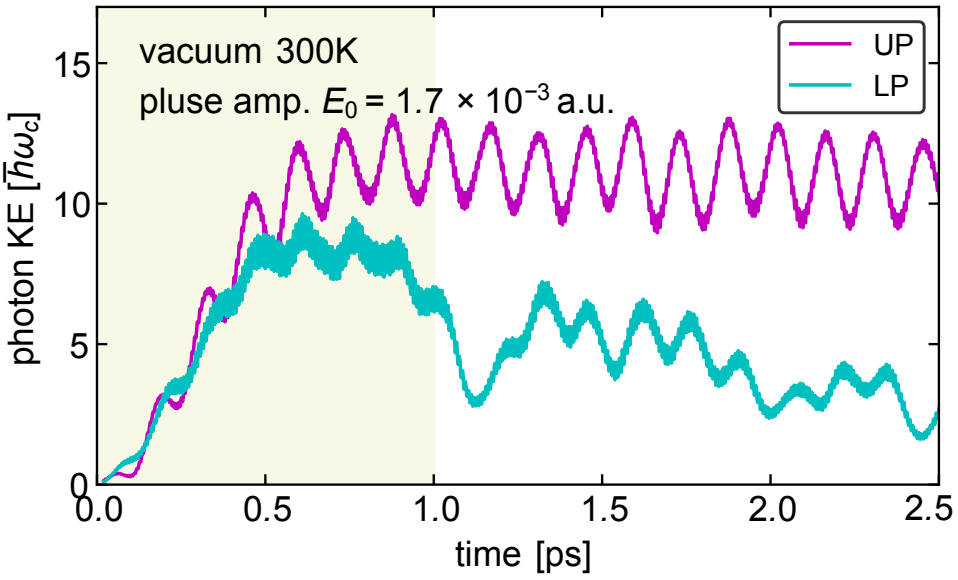

Figure S1: Kinetic energy dynamics of cavity photons under Gaussian pumping of the UP (magenta curve) or LP (cyan curve) in the absence of n-dodecane solvent molecules. All simulation conditions are the same as Fig. 3a except here the solvent molecules are not included (i.e., the simulation is performed for the solute in vacuum). Compared with Fig. 3a in the main text, excluding n-dodecane solvent molecules significantly slows down the UP dephasing but has less impact on the LP dephasing.

4. Benchmark of single-molecule reaction under VSC

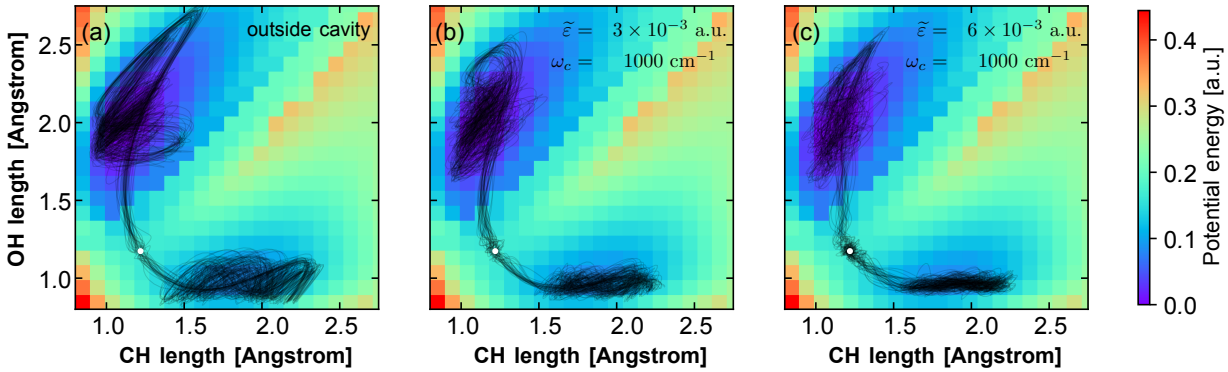

Figure S2: VSC effects on single-molecule isomerization reaction: $CH_2O \longleftrightarrow CHOH$. The molecule starts at the transition state (the white dot in each plot), and the cavity frequency is $\omega_c = 1000$ cm^{-1}. The molecule is (a) decoupled from the cavity or (b,c) coupled to the cavity with light-matter coupling strength (b) $\widetilde{\varepsilon} = 3 \times 10^{-3}$ a.u. or (c) $\widetilde{\varepsilon} = 6 \times 10^{-3}$ a.u. Each thin black line represents a molecular trajectory when the initial velocities are sampled from a Maxwell–Boltzmann distribution at 300 K, and 64 trajectories are sampled per panel. Under VSC, the molecular trajectory spends more time near the transition state, in agreement with a recent model study of the dynamical caging effect.[S9] Note that this study is used to benchmark the functionality of CavMD and should not be used to interpret recent VSC experiments on chemical catalysis in the collective regime. A tutorial on running this calculation is also available at `https://github.com/TaoELi/cavity-md-ipi`. Psi4[S10] is used to perform on-the-fly gradient evaluations at the level of Hartree–Fock theory with a 6-31G* basis set.

References

[S1] Becke, A. D. Density-Functional Exchange-Energy Approximation with Correct Asymptotic Behavior. *Phys. Rev. A* **1988**, *38*, 3098.

[S2] González-Blanco, O.; Branchadell, V. Density functional study of the Fe–CO bond dissociation energies of Fe(CO)5. *J. Chem. Phys.* **1998**, *110*, 778.

[S3] Jang, J. H.; Lee, J. G.; Lee, H.; Xie, Y.; Schaefer, H. F. Molecular Structures and Vibrational Frequencies of Iron Carbonyls: Fe(CO)5, Fe2(CO)9, and Fe3(CO)12. *J. Phys. Chem. A* **1998**, *102*, 5298–5304.

[S4] Grimme, S.; Brandenburg, J. G.; Bannwarth, C.; Hansen, A. Consistent Structures and Interactions by Density Functional Theory with Small Atomic Orbital Basis Sets. *J. Chem. Phys.* **2015**, *143*, 054107.

[S5] Jorgensen, W. L.; Maxwell, D. S.; Tirado-Rives, J. Development and Testing of the OPLS All-Atom Force Field on Conformational Energetics and Properties of Organic Liquids. *J. Am. Chem. Soc.* **1996**, *118*, 11225–11236.

[S6] Vreven, T.; Morokuma, K. *Annu. Rep. Comp. Chem.*; Elsevier, 2006; Vol. 2; pp 35–51.

[S7] Hirshfeld, F. L. Bonded-atom Fragments for Describing Molecular Charge Densities. *Theor. Chim. Acta* **1977**, *44*, 129–138.

[S8] Martínez, L.; Andrade, R.; Birgin, E. G.; Martínez, J. M. PACKMOL: A Package for Building Initial Configurations for Molecular Dynamics Simulations. *J. Comput. Chem.* **2009**, *30*, 2157–2164.

[S9] Li, X.; Mandal, A.; Huo, P. Cavity Frequency-Dependent Theory for Vibrational Polariton Chemistry. *Nat. Commun.* **2021**, *12*, 1315.

[S10] Smith, D. G. A. et al. Psi4 1.4: Open-Source Software for High-Throughput Quantum Chemistry. *J. Chem. Phys.* **2020**, *152*, 184108.